ANISOTROPY VS CHEMICAL COMPOSITION AT ULTRA-HIGH ENERGIES

Martin Lemoine[1]
Institut d'Astrophysique de Paris,
CNRS, Université Pierre & Marie Curie,
98 bis boulevard Arago, F-75014 Paris, France

Eli Waxman[2]
Physics Faculty,
Weizmann Institute,
Rehovot 7600, Israel
Draft version October 31, 2018

ABSTRACT

This paper proposes and discusses a test of the chemical composition of ultra-high energy cosmic rays that relies on the anisotropy patterns measured as a function of energy. In particular, we show that if one records an anisotropy signal produced by heavy nuclei of charge Z above an energy E_{thr}, one should record an even stronger (possibly much stronger) anisotropy at energies $> E_{\mathrm{thr}}/Z$ due to the proton component that is expected to be associated with the sources of the heavy nuclei. This conclusion remains robust with respect to the parameters characterizing the sources and it does not depend at all on the modelling of astrophysical magnetic fields. As a concrete example, we apply this test to the most recent data of the Pierre Auger Observatory. Assuming that the anisotropy reported above 55 EeV is not a statistical accident, and that no significant anisotropy has been observed at energies $\lesssim 10$ EeV, we show that the apparent clustering toward Cen A cannot be attributed to heavy nuclei. Similar conclusions are drawn regarding the apparent excess correlation with nearby active galactic nuclei. We then discuss a robust lower bound to the magnetic luminosity that a source must possess in order to be able to accelerate particles of charge Z up to 100 EeV, $L_B \gtrsim 10^{45} Z^{-2}$ erg/s. Using this bound in conjunction with the above conclusions, we argue that the current PAO data does not support the model of cosmic ray origin in active radio-quiet or even radio-loud galaxies. Finally, we demonstrate that the apparent clustering in the direction of Cen A can be explained by the contribution of the last few gamma-ray bursts or magnetars in the host galaxy thanks to the scattering of the cosmic rays on the magnetized lobes.

Subject headings: cosmic rays

1. INTRODUCTION

The sources of ultra-high energy cosmic rays have remained elusive in spite of the enormous progress reached on the experimental side, with present day detectors reaching apertures $> 10\,000\,\mathrm{km}^2$ sr yr. The differential energy spectrum, the chemical composition and the distribution of arrival directions on the sky are as many clues to the nature of the source. There is now a consensus on the existence of the GZK cut-off (Greisen 1966; Zatsepin & Kuz'min 1966), which has been observed by two different experiments (Abbasi et al. 2008, Abraham et al. 2008a). The existence of this GZK cut-off puts on solid ground the models which attribute the origin of ultra-high energy cosmic rays to powerful astrophysical objects distributed on cosmological scales, such as powerful radio-galaxies (Rachen & Biermann 1993), gamma-ray bursts (Milgrom & Usov 1995, Vietri 1995, Waxman 1995), or magnetars (Arons 2003).

Experimental results on the chemical composition and anisotropies are however far more confusing. While the most recent analysis of HiRes data points to a proton composition above the ankle (Abbasi et al. 2005, Belz 2009), the fluorescence data of the Pierre Auger Observa-

tory (PAO) rather indicates an increasingly heavier composition above this energy, with the last data points at $\sim 30 - 50$ EeV close to expectations for iron (Unger et al. 2007, Wahlberg et al. 2009). Regarding the distribution of arrival directions on the sky, there exist various contradictory claims, see for instance the correlation with the super-galactic plane reported by Stanev et al. (1995), contradicted by the results of the AGASA experiment (Takeda et al. 1999); the claim for a correlation with BL Lac objects in Tinyakov & Tkachev (2001, 2002), Gorbunov et al. (2002, 2004), which has been debated (Evans, Ferrer & Sarkar 2003, 2004; Tinyakov & Tkachev 2004); as well as the possible detections of multiplets in various datasets, e.g. Takeda et al. (1999), Uchihori et al. (2000), Farrar, Berlind & Hogg (2006), the significance of which is questioned in Abbasi et al. (2004) and Finley & Westerhoff (2004); or, finally, the recent data of the PAO, which reveal a correlation with nearby active galactic nuclei (AGN), the maximal signal being obtained for a search radius of $3.1°$ around AGN located closer than 75 Mpc and for energies above 57 EeV (Abraham et al. 2007, 2008b).

In general, these issues of anisotropies and chemical composition are discussed separately. However, as we argue in the present paper, one can construct a powerful test of the chemical composition by using the anisotropy

---

[1] email: lemoine@iap.fr
[2] email: eli.waxman@weizmann.ac.il

signal at various energies. This becomes particularly interesting when one notes that measurements of chemical composition are relatively sensitive to the details of the shower reconstruction, in particular to the extrapolation of hadronic models at energies beyond those currently tested in accelerators (see Wibig 2008, Ulrich et al. 2009a,b and Wibig 2009 for recent discussions of this issue). Moreover, measurements of chemical composition rely on the use of fluorescence detectors whose duty cycle is rather low and cannot be made event by event, so that they are limited by statistics.

The essence of the test proposed in this paper is to exploit the fact that a source in the sky emitting heavy nuclei of charge Z at an energy E is expected to produce a similar anisotropy pattern at energies E/Z via the proton component which is expected to be associated with the same source. Our expectation for the existence of a proton component relies on the theoretical expectation, that if protons are present in the plasma in which particle acceleration takes place, then they should be accelerated along side with the heavy nuclei. As discussed in some detail at the end of § 2, a source accelerating heavy nuclei to energy E is quite generally expected to accelerate protons to energy E/Z. Although the isotropic background "noise" increases at lower energies, we show in § 2 that the signal-to-noise ratio for the detection of the anisotropy also increases. This prediction does not depend at all on the modelling of astrophysical magnetic fields as it only relies on the property that protons of energy E/Z follow the same path in the intervening magnetic fields and produce the same angular image as heavy nuclei of charge Z and energy E. The proposed test is discussed in more detail in Section 2. When applied to the most recent data of the PAO (Section 3), it shows that the signal that is responsible for the apparent anisotropy pattern at energies $> 55 \, \mathrm{EeV}$ must not be heavy but light nuclei, provided this anisotropy is confirmed by future data, and provided the PAO does not see evidence for anisotropy at lower energies, as seems to be the case (Abraham et al. 2007).

We discuss the implications of these results in the last two Sections. In Section 4, we argue that local AGN (including FR I radio-galaxies) do not possess the power required to accelerate protons to ultra-high energies. When combined with the previous conclusions, this leads to the conclusion that the current PAO data do not support AGN as sources of the highest energy cosmic rays. Finally, Section 5 summarizes the findings and concludes that the current data on composition and anisotropy suggest one of the following: (i) the shower modelling or, what would be more interesting, the hadronic theoretical models of shower reconstruction are in error at high energy; (ii) the composition switches abruptly from heavy to light above $30 - 50 \, \mathrm{EeV}$; (iii) the source injects primarily heavy nuclei (which seems unlikely); (iv) the anisotropy seen by the PAO is a statistical artefact.

2. TESTING THE CHEMICAL COMPOSITION OF ULTRA-HIGH ENERGY COSMIC RAYS WITH ANISOTROPY DATA

As argued below, one can use the results of searches for anisotropy at various energies in order to constrain the chemical composition of ultra-high energy cosmic rays. The basic claim is the following: if one detects anisotropy above some energy E_{thr}, but not below, then the chemical composition is most likely light above E_{thr}, because one would have otherwise observed a similar anisotropy pattern at an energy E_{thr}/Z, with Z the assumed average charge of the cosmic rays at energies $> E_{\mathrm{thr}}$.

Consider a region of the sky, of angular size θ and solid angle $\Delta\Omega = 2\pi(1 - \cos\theta)$, showing an excess of particles above isotropic expectations above some energy threshold E_{thr}. The most natural interpretation is to infer the existence of one or more sources in this direction, the image of which is spread over $\Delta\Omega$, because of smearing by θ in the intervening magnetic fields, or because $\Delta\Omega$ subtends the source distribution. For the sake of the argument, we assume that the spectrum produced by the source consists of protons and of heavy nuclei of charge Z. In all known source models, one expects that the ratio of the elemental spectra $q_p(E)/q_Z(E) > 1$ and more generally $q_p(E)/q_Z(E) \gg 1$ at a given energy $E \ll E_{\max}(p)$, where $E_{\max}(p)$ denotes the maximal energy at the source for protons. For instance, the composition ratio of protons to iron peak elements ($Z \geq 17$) in the Galactic cosmic ray spectrum, which is roughly consistent with the solar abundance when compared at a given energy per nucleon, implies a source composition at a given energy $q_p : q_{Z \geq 17} \simeq 1 : 0.06$ (as taken from the recent ATIC-2 data, Panov et al. 2006). The only energy regime in which one may obtain $q_p(E)/q_Z(E) \ll 1$ is $E_{\max}(p) \ll E \ll E_{\max}(Z)$, with $E_{\max}(Z)$ the maximal energy for the nuclei of charge Z (see also further below). We also assume here that the maximal energy scales as Z; as argued further below, this is a conservative choice. Now, let us ask what would be seen if the composition above E_{thr} were heavy. Consider the quantity

$$\Sigma_Z(> E_{\mathrm{thr}}) \equiv \frac{\Delta N(> E_{\mathrm{thr}})}{\sqrt{N_{\mathrm{iso}}(> E_{\mathrm{thr}})}} \, , \qquad (1)$$

which characterizes the signal-to-noise ratio of the anisotropy signal: $\Delta N(> E_{\mathrm{thr}})$ represents the excess number of events over isotropic expectations, i.e. the difference between the total number of events observed above E_{thr} within $\Delta\Omega$ and $N_{\mathrm{iso}}(> E_{\mathrm{thr}})$, the number of events expected from the isotropic background. In the above model, $\Delta N(> E_{\mathrm{thr}})$ corresponds on average to the number of events produced by the sources inside $\Delta\Omega$. A detection of anisotropy thus corresponds to $\Sigma_Z(> E_{\mathrm{thr}}) \gg 1$.

One can now compute a similar quantity, but corresponding to the proton component at energies $> E_{\mathrm{thr}}/Z$, denoted $\Sigma_p(> E_{\mathrm{thr}}/Z)$. These protons have a same magnetic rigidity than the heavy component above E_{thr}, therefore they follow the same path in the Galactic and extra-galactic magnetic fields, and consequently they are to produce a similar anisotropy pattern in the sky, up to the composition ratio of the elemental spectra and up to the level of background noise associated with the isotropic component. Assuming that the elemental spectra at injection have the same power-law form $q_i(E) \propto E^{-s}$ at $E \ll E_{\max}(Z_i)$, and that the total number of events observed scales as $E^{1-s_{\mathrm{obs}}}$, with s_{obs} the slope of the observed all-sky differential spectrum,

one finds

$$\Sigma_p(> E_{\mathrm{thr}}/Z) = \Sigma_Z(> E_{\mathrm{thr}})\frac{q_p(E_{\mathrm{thr}}/Z)}{q_Z(E_{\mathrm{thr}}/Z)}\,\alpha_{\mathrm{loss}}\,Z^{s-(s_{\mathrm{obs}}+1)/2}\,.$$

(2)

The fudge factor $\alpha_{\mathrm{loss}} \gtrsim 1$ incorporates the effect of energy losses; it is discussed in more detail in the following. At energies above the ankle, one has $s_{\mathrm{obs}} \simeq 2.7$ (Abbasi et al. 2008, Abraham et al. 2008a). Therefore, if the source emits a power-law with $s = 2$, one finds that the signal-to-noise ratio for detecting the anisotropy is larger at E_{thr}/Z than at E_{thr} by a factor $\approx \alpha_{\mathrm{loss}} Z^{0.2} q_p(E_{\mathrm{thr}}/Z)/q_Z(E_{\mathrm{thr}}/Z)$, generally expected to be significantly larger than unity! Clearly, the softer the source spectrum, the larger the gain in signal-to-noise ratio with decreasing Z.

The factor α_{loss} accounts for the difference between the propagated and injected spectra. Given that the energy loss distance for protons of energy E_{thr}/Z is much larger than the energy loss distance for heavy nuclei of energy E_{thr}, if $E_{\mathrm{thr}} \gtrsim 10^{19}\,\mathrm{eV}$, one expects $\alpha_{\mathrm{loss}} > 1$. Indeed, regarding the (primary) proton component, energy losses can be safely neglected at E_{thr}/Z energies, since the attenuation length is of order of a Gpc or more at EeV energies, which is much larger than the depth up to which anisotropies can be produced, this latter being of order of the inhomogeneity scale of the large scale structure $\sim 100\,\mathrm{Mpc}$ or of the distance to the closest source, whichever is larger. Therefore, α_{loss} approximately corresponds to the reciprocal of the attenuation factor for heavy nuclei of charge Z and energy $> E_{\mathrm{thr}}$ propagating over the distance scale l to the sources inside $\Delta\Omega$. The attenuation factor is understood as the ratio of the flux above $> E_{\mathrm{thr}}$ after propagation on a distance l to the injected flux above this energy. For the case of iron primaries, this attenuation factor is 0.7 above 55 EeV at a distance of 10 Mpc, becoming 0.4 at a distance of 100 Mpc (counting in the propagated flux all secondary nuclei with $Z > 17$). For oxygen, the attenuation factor is 0.5 at 10 Mpc, becoming 0.1 at 100 Mpc (counting in all C, N and O secondary nuclei); see Bertone et al. (2002) for an illustration of the relative fragility of ultra-high energy CNO nuclei vs iron peak elements.

Actually, this enhancement factor α_{loss} should be further increased by the number of secondary protons with energy $> E_{\mathrm{thr}}/Z$ produced by the photo-disintegration of the primary heavy nuclei with energy $> E_{\mathrm{thr}}$. This number is not easy to quantify but it can be significant. For instance, recent simulations by Aloisio, Berezinsky & Gazizov (2008) indicate that the signal should be dominated by protons at energies $> 1-2 \times 10^{19}\,\mathrm{eV}$ even if the source composition were strongly enriched in iron nuclei [assuming of course that $E_{\mathrm{max}}(p) > 3 \times 10^{19}\,\mathrm{eV}$]. Allard et al. (2008) also conclude that heavy nuclei could be found in abundance at the detector only if the composition were essentially dominated by Fe group nuclei at energies beyond $10^{20}\,\mathrm{eV}$. As discussed in this latter reference, and above, the generic case that gives rise to a heavy composition at ultra-high energies is when the proton maximal energy at the source is smaller than the GZK cut-off. In the following, we adopt a conservative point of view and neglect the effect of energy losses, i.e. we set $\alpha_{\mathrm{loss}} = 1$.

Let us now discuss the scaling of E_{max} with charge.

The maximal energy is given by the comparison of the acceleration timescale (which depends on rigidity E/Z) with the minimum of the escape timescale (which also depends on E/Z), the age of the source or dynamical timescale (which do not depend on E, Z) and the energy losses timescale (which depends on E, Z and mass number A). If the latter timescale does not provide the dominant limitation to the acceleration mechanism, then the maximal energy scales as the rigidity, as assumed above. If energy losses are dominant however, one expects $E_{\mathrm{max}}(Z) \lesssim ZE_{\mathrm{max}}(p)$, as explained in the following. Then the above argument would remain valid, as it only requires that protons exist at energies $> E_{\mathrm{thr}}/Z$, i.e. that $E_{\mathrm{max}}(p) \gtrsim E_{\mathrm{thr}}/Z$. Note that in the more extreme case in which protons and heavy nuclei had similar maximal energies, the composition at ultra-high energies $> E_{\mathrm{thr}}$ would be dominated by protons, and therefore the anisotropy would be due to those protons since they have a higher rigidity than the heavy nuclei of a same energy. For photo-hadronic interactions, the energy loss timescales for protons and iron-peak nuclei are known to be comparable, while that of intermediate elements is generally smaller; in that case, one would expect $E_{\mathrm{max}}(p) \sim E_{\mathrm{max}}(\mathrm{Fe}) \gtrsim E_{\mathrm{max}}(Z \sim 10)$. Regarding synchrotron losses, the energy loss timescale scales as $(Z/A)^{-4}E^{-1}$, therefore $E_{\mathrm{max}} \propto Z^{1/2}(Z/A)^{-2}$ if the acceleration timescale $t_{\mathrm{acc}} \propto E/Z$ and synchrotron losses dominate at the highest energies. In that case, the scaling $E_{\mathrm{max}}(Z)/E_{\mathrm{max}}(p) \propto Z$ remains correct to within a factor of order unity. The above conclusions agree with the recent simulations of Allard & Protheroe (2009).

Finally, accounting for a more complex chemical composition with more than two species would not modify significantly the results shown in Eq. (1) as long as the anisotropy above E_{thr} is indeed due to the species of charge Z. In practice, it will be useful to test the composition above E_{thr} by checking the anisotropies at various E_{thr}/Z_i, with $Z_i = 2, 8, 14, 26$ representative of the most abundant elements.

In the following, we provide specific examples of the above test applied to the most recent data of the PAO. We will show in particular that the above argument remains valid when one considers the all-sky anisotropy pattern due to an ensemble of close-by sources.

3. APPLICATION TO THE PIERRE AUGER DATA

Abraham et al. (2007, 2008b) have reported a correlation of 20/27 arrival directions of the highest energy events ($E > 5.7 \times 10^{19}\,\mathrm{eV}$) with nearby ($d < 75\,\mathrm{Mpc}$) active galactic nuclei. However, the typical model of ultra-high energy cosmic ray origin in AGN refers to strongly beamed Fanaroff-Riley II (FR II) sources with giant radio lobes (e.g. Rachen & Biermann 1993), while 19 out of these 20 correlating AGN in the Pierre Auger dataset belong to the Seyfert or LINER class, only one being a Fanaroff-Riley I (FR I) radio-galaxy (Cen A). These correlating AGNs are thus more likely to be tracers of the local large scale structure in which the actual sources of ultra-high energy cosmic rays camouflage and indeed, the arrival directions are compatible with a distribution of sources following the large scale structure (Kashti & Waxman 2008, Ghisellini et al. 2008, Zaw, Farrar & Greene 2009). The extended dataset up to 2009 of the PAO reveals a significantly weaker correla-

tion, with only 26 out of 58 events above 55 EeV lying within 3.1° of an AGN located within 75 Mpc (Hague et al. 2009). This level of correlation is compatible with that expected for sources distributed as the large scale structure (see discussion in Kotera & Lemoine 2008 and Aublin et al. 2009 for a detailed discussion of the correlation with cosmological catalogs). It is important to note that the departure from isotropy lies at the 1% level. Therefore one should be careful not to overinterpret this excess. In the following, we use these PAO results as a concrete example for the test developed in the previous section.

Interestingly, the PAO data up to 2007 has also shown evidence for clustering of events in the region around Cen A, with as many as 9 events within 20° (Gorbunov et al. 2008), as well as correlation of 8 out of 27 events with a sample of radio-galaxies (Moskalenko et al. 2008; Nagar & Matulich 2008). This has triggered a surge of interest in models of ultra-high energy cosmic ray origin in Cen A as well as forecast studies of neutrino and gamma-ray expected signals from Cen A (e.g. Cuoco & Hannestad 2008, Gupta 2008, Halzen & O'Murchadha 2008, Holder et al. 2008, Kachelriess et al. 2008). However, such a correlation does not necessarily imply that Cen A is the source of these cosmic rays. First of all, and as noted in Abraham et al. (2008b), Hague et al. (2009), the evidence for clustering is based on an a posteriori analysis, so that it is difficult to quantify the level of significance. Even if future data confirm this clustering, one must keep in mind that Cen A lies in front of one of the largest concentrations of matter in the local Universe, at ∼ 50 Mpc from us, so that the correlation could be accidental. Finally, as we argue in Section 4.2, the Cen A AGN/jet/lobe system is too weak to accelerate protons up to the observed energies > 57 EeV.

Even more intriguing is the fact that the chemical composition measured by the PAO becomes increasingly heavier above the ankle at 4 EeV, with the last data points at $30 - 50$ EeV lying close to expectations for iron (Unger et al. 2007, Wahlberg et al. 2009). Such a measurement is in obvious conflict with the most recent analysis of HiRes data, which indicate a pure proton composition up to 30 EeV (Belz 2009). As we argue in the following, it is also at odds with the observed anisotropy pattern above 55 EeV, unless the composition abruptly changes from heavy to light above $30 - 50$ EeV.

3.1. Anisotropy towards Cen A

Let us first discuss the anisotropy toward Cen A, using the most recent PAO dataset, in particular, 12 events located within 18° out of a total of 58 events above 55 EeV (Hague et al. 2009), assuming that the clustering is not a statistical accident. In a first approximation, one can model the anisotropy pattern as in the previous section, with one (or several clustered) source(s) contributing a fraction x of the total flux, the remaining $1 - x$ being accounted for by an isotropic background. We do not need to assume that Cen A itself is a source, but we center the anisotropic signal on the location of Cen A in order to match the observed pattern. Given that 2.7 events are expected on average from this region of the sky if the sources are distributed isotropically, we set $x = 0.15$ in the following.

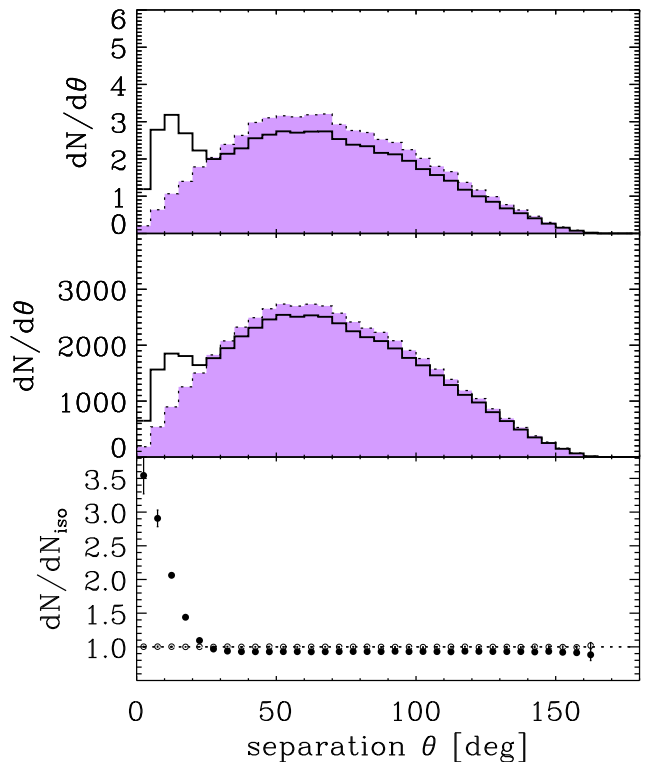We   assume   that   the   sources   inject   pro-

FIG. 1.— Top panel: differential histogram of the number of events above 55 EeV as a function of the angular separation to Cen A, in solid line for the model described in the text (sources contributing 15% of the flux, forming an image of size $\delta\theta = 10°$, superimposed on an isotropic background) and expected signal from an isotropic population of sources (colored region). The flux is normalized to a total of 58 events above 55 EeV. Middle panel: same histogram but for $E > 2.2$ EeV, assuming that the high energy events are iron nuclei and that protons are injected with composition ratio $q_p(E) : q_Z(E) = 1 : 0.06$ at $E < 3$EeV. The anisotropy signal is much stronger, as measured by the number of events in each bin. Bottom panel: in filled circles, the ratio of the differential histogram shown in the middle panel to the isotropic expectations $dN_{iso}/d\theta$ with error bars estimated through the Monte Carlo; in empty circles, the same histogram but for a model assuming that the high energy events are protons only and $\delta\theta \propto (E/Z)^{-1}$. Only the latter model is compatible with an isotropic distribution of arrival directions at energies > 2.2 EeV.

tons   and   iron   nuclei   with   powerlaw   spectra $q_Z(E) \propto E^{-s} \exp\{-E/[ZE_{max}(p)]\}$, producing an angular image of size $\delta\theta$. As before, this angle could represent smearing due to angular deflection, in which case $\delta\theta \propto (E/Z)^{-1}$, or the angular size of the ensemble of sources. Although we assume that all heavy nuclei are iron, the following could be easily generalized to any kind of mixed composition without changing the basic result. We also neglect the energy losses for the spectrum of the anisotropic component, as before. This is motivated by the proximity of matter in this direction of the sky and, as discussed before, incorporating energy losses would not diminish the signal we are to extract out of the data, while it would introduce other free parameters. The remaining $1 - x$ fraction of the flux is modelled with an isotropic background, e.g. as produced by far away sources.

Let us first assume that the composition is dominated by iron at the highest energies. We set $E_{thr} = 55$ EeV, and $\delta\theta = 10°$ above E_{thr}. We also set $E_{max}(p) = 3$ EeV, so that essentially no proton contribute to the signal

above E_{thr}. In the top panel of Fig. 1 we plot the histogram of the number of events as a function of the angular distance to the source (solid line). The colored region indicates the expectations for a purely isotropic signal. The departure from isotropy is clear, although the uncertainty on the signal in each bin is substantial given the small number of events involved. Here the number of events within $18°$ of Cen A is $\simeq 9$ for the model (slightly lower than the observed 12 events, yet within the uncertainty) and 2.7 for the isotropic expectations so that the inferred $\Sigma_{\mathrm{Fe}}(> 55\,\mathrm{EeV}) = \Delta N/\sqrt{N_{\mathrm{iso}}} \simeq 5.5$.

In the middle panel of Fig. 1, we plot the same histogram, but at an energy $E_{\mathrm{thr}}/26 = 2.2\,\mathrm{EeV}$. In order to simulate the anisotropy signal, we have proceeded as follows. We have assumed that the total number of events increases (with decreasing energy) according to the observed data (in particular the PAO spectrum published in Yamamoto et al. 2007), and we have calculated the contribution to this flux above $E_{\mathrm{thr}}/26$ for all the protons injected by the source above this energy. We have assumed that the ratio of protons to iron is 1:0.06 at a given energy well below E_{max}, corresponding to the composition ratio of proton to iron peak elements ($Z \geq 17$) in the galactic cosmic ray spectrum reconstructed at the source. The iron nuclei injected by the source at energies $\gtrsim 2.2\,\mathrm{EeV}$ add up to the isotropic background and do not contribute to the anisotropy signal. As made obvious in Fig. 1, the gain in signal-to-noise ratio is very large: the number of events observed above $2.2\,\mathrm{EeV}$ within $18°$ is now 5150, for 2330 expected, so that $\Sigma_p(> 2.2\,\mathrm{EeV}) = \Delta N/\sqrt{N_{\mathrm{iso}}} \simeq 100$. This gain by a factor $\simeq 20$ can be recovered from Eq. (2).

Finally, the lower panel of Fig. 1 shows the ratio of the differential histograms $dN/d\theta$ for the source proton contribution plus isotropic background (filled circles) to the isotropic background $dN_{\mathrm{iso}}/d\theta$ normalized to a same total number of events, including the error bars evaluated through the Monte Carlo simulation. The empty circles show the same quantity, but for a model in which the source injects only protons, even up to the highest energies, assuming that $\delta\theta$ represents magnetic deflection, i.e. $\delta\theta \propto (E/Z)^{-1}$: we have set $\delta\theta = 10°$ above $55\,\mathrm{EeV}$ in this model, so that the anisotropy signal above $55\,\mathrm{EeV}$ is similar to that of the previous iron+proton model shown in the top panel of Fig. 1, but the low energy signal is essentially isotropic, see the bottom panel.

The conclusions to be drawn are clear. If the clustering seen toward Cen A is real, the events responsible for this anisotropy pattern toward Cen A above $55\,\mathrm{EeV}$ are unlikely to be heavy nuclei, otherwise PAO would have observed a much stronger anisotropy at energies $< 40\,\mathrm{EeV}$ (Abraham et al. 2007, 2008b).

3.2. Correlation with the Véron-Cetty & Véron (2006) catalog of AGN

In the present Section, we investigate how the anisotropy signal with respect to nearby AGN, as reported in Hague et al. (2009) can be used to discriminate the chemical composition at the highest energies. We proceed in a similar way as before, but we now assume that the spectrum is composed of two components: one that follows the local large scale structure, contributing a fraction x to the flux above $55\,\mathrm{EeV}$, and one isotropic component that makes up for the remainder, $1 - x$. As a
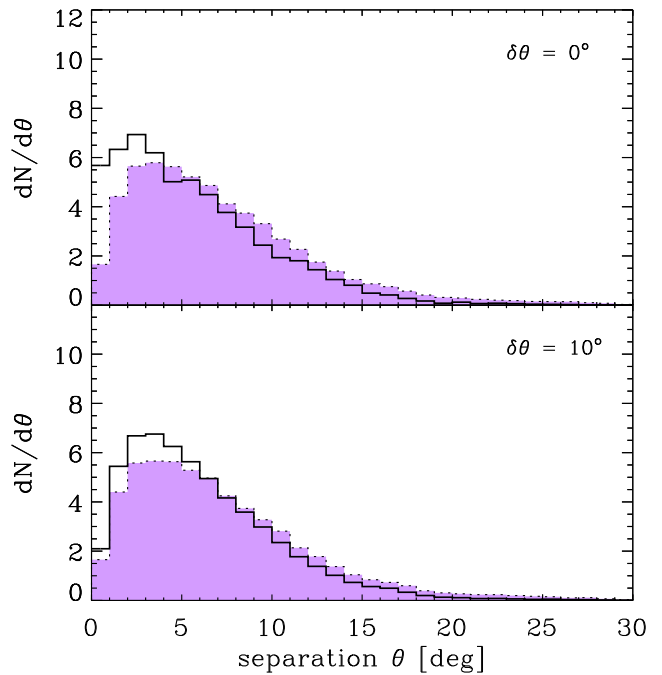

FIG. 2.— Differential histograms of the number of events above 55 EeV as a function of the angular separation to the closest AGN, drawn from the Véron-Cetty & Véron (2006) catalog up to a distance of 75 Mpc. The solid line corresponds to the model in which 90% of the flux above 55 EeV is produced by sources distributed as the large scale structure, modeled through the PSCz catalog of galaxies, smeared by a deflection angle $\delta\theta$, as indicated. The colored region indicates the expectation for purely isotropic arrival directions. The histograms are normalized to a total of 58 events, as observed by PAO.

proxy for the local large scale structure, we use the PSCz catalog of galaxies (Saunders et al. 1991), as in previous studies (Kashti & Waxman 2008, Kotera & Lemoine 2008). Out of simplicity, we assume that the sources follow the PSCz distribution without bias. However, we allow for the possibility of a deflection angle $\delta\theta$ in intervening magnetic fields and we explore two possible values $\delta\theta = 0°$ and $\delta\theta = 10°$ above 55 EeV. This choice is motivated by the resolution of the PSCz catalog, approximately $7°$, and by the possibility that this signal is composed of heavy nuclei. In practice, we proceed through Monte Carlo simulations as follows. We construct many mock catalogs of angular sky distributions, each mock catalog being a sample of 58 events above 55 EeV (or the corresponding number at any other energy). The arrival direction of each event in the sample is drawn at random, according to a probability law reproducing the PSCz distribution and PAO coverage if it belongs to the x anisotropic fraction, or reproducing isotropic arrival directions and PAO coverage if the event belongs to the remaining $1 - x$ fraction of isotropic background. In order to draw an event from the PSCz catalog, we include the appropriate weight factors for the flux dilution with inverse distance squared, for the PSCz exposure function and for the PAO aperture. Then we randomly displace this arrival direction by $\delta\theta$ in the plane of the sky. The energy losses are accounted for by the depth of the catalog, which is limited to 200 Mpc.

We have set $x = 0.90$, which allows to produce an anisotropy signal close to the level observed: the PAO
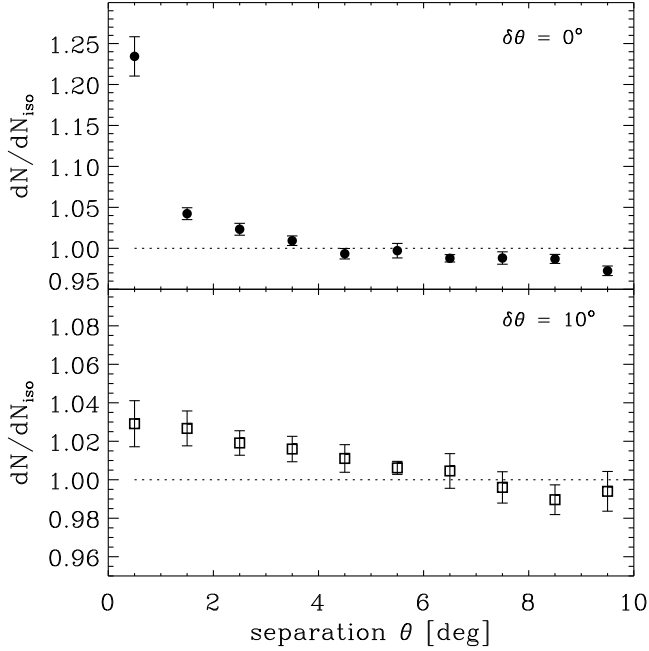
FIG. 3.— Ratio of the differential histograms for the models shown in Fig. 2 to histograms for purely isotropic arrival directions, but computed from the proton component at energies > 2.2 EeV. The uncertainties measured through the Monte Carlo are indicated. Note the change of scale between the two panels corresponding to the two values of $\delta\theta$, as indicated.

indeed records 24 events out of 58 events above 55 EeV located within 3° of an AGN closer than 75 Mpc, while the above model produces 19 events within 3° if $\delta\theta = 0°$ and 14 events if $\delta\theta = 10°$. The model with 90% of the flux above 55 EeV coming from sources distributed as the large scale structure with negligible deflection thus gives a number of correlating AGN within 3° that is comparable to that seen by PAO, to within the uncertainty. A deflection angle $\delta\theta = 10°$ provides a signal that is marginally too low, but given the simplifying assumptions made above, this is not crucial. It certainly indicates that larger deflection angles will probably result in too small anisotropies. It is interesting to note that the anisotropy signal peaks at a separation which is substantially smaller than $\delta\theta$, i.e. $\sim 4 - 5°$ for $\delta\theta = 10°$. This of course results from the PAO procedure, which selects the closest AGN to the arrival direction and not to the source direction, i.e. after the direction at the source has been modified by $\delta\theta$. The differential histograms corresponding to these models and isotropic expectations are shown in Fig. 2 as a function of the angular separation to the closest AGN drawn from the Véron-Cetty & Véron (2006) catalog, with an arbitrary cut at 75 Mpc, following the PAO analysis. These histograms are shown for the two possible values of $\delta\theta$, as indicated. Here, we find $\Sigma_{\rm Fe}(> 55\,{\rm EeV}) \simeq 2.1$ and 0.76 for $\delta\theta = 0°$ and $\delta\theta = 10°$ respectively. The signal is thus marginal in terms of departure from isotropy.

We now plot the ratios of the differential histograms expected in these two models at low energy > 2.2 eV to the histogram expected for purely isotropic arrival directions, as before. We have assumed a conservative composition ratio 1:0.06 between proton and iron as in the previous section, and we have neglected energy

losses on the propagated spectra. The results are shown in Fig. 3, which clearly reveals a stronger anisotropy signal at these energies. In terms of signal-to-noise, we find $\Sigma_p(> 2.2\,{\rm EeV}) \simeq 6.2$ and 2.3 respectively for $\delta\theta = 0°$ and $\delta\theta = 10°$ ($\Delta N = 623$ and 235 respectively, $N_{\rm iso} = 10100$), which significantly exceed the signal-to-noise ratios obtained above 55 EeV. This generalizes the argument presented in Section 2 for the case of a more complex distribution of point sources on the sky, superimposed on an isotropic background. It also shows that the present angular data of the PAO disfavors a heavy composition at ultra-high energies. Strictly speaking, this test demonstrates that the *anisotropic* part of the signal cannot be due to heavy nuclei *but* one cannot exclude that the isotropic background is made up of heavy nuclei. However, our above model also suggests that a significant fraction (90% in Fig. 2,3) of the flux at > 55 EeV is produced by the anisotropic component if one takes at face value the anisotropy results of the PAO. This suggests that the bulk of ultra-high energy cosmic rays above 55 EeV are protons.

4. AGN AS SOURCES OF ULTRA-HIGH ENERGY COSMIC RAYS?

4.1. *AGN luminosity vs acceleration*

On general grounds, one can construct a lower bound to the magnetic luminosity that a source must exhibit in order to be able to accelerate particles up to 10^{20} eV (Norman et al. 1995, Waxman 1995, Lyutikov & Ouyed 2005, Waxman 2005). Let us first briefly describe the general, model independent argument given in Waxman (1995). Consider an astrophysical source driving a flow of magnetized plasma, with characteristic magnetic field strength B and velocity v. Imagine now a conducting wire encircling the source at radius R. The potential generated by the moving plasma is given by the time derivative of the magnetic flux, and is therefore given by $V = \beta B R$ where $\beta = v/c$. A proton which is allowed to be accelerated by this potential drop would reach energy $E_p \sim \beta e B R$. The situation is somewhat more complicated in the case of a relativistic outflow, where $\Gamma \equiv (1 - \beta^2)^{-1/2} \gg 1$. In this case, the proton is allowed to be accelerated only over a fraction of the radius R, comparable to R/Γ. To see this, one must realize that as the plasma expands, its magnetic field decreases, so the time available for acceleration corresponds, say, to the time of expansion from R to $2R$. In the observer frame this time is R/c, while in the plasma rest frame it is $R/\Gamma c$. Thus, a proton moving with the magnetized plasma can be accelerated over a transverse distance $\sim R/\Gamma$. This sets a lower limit to the product of the magnetic field and source size, which is required to allow acceleration to E_p, $BR > \Gamma E_p/e\beta$. This also sets a lower limit to the rate L_B at which energy is carried by the out flowing plasma, and which must be provided by the source (Waxman 1995, 2005),

$$L_B > \frac{\Gamma^2}{\beta}\left(\frac{E}{Ze}\right)^2 c = 10^{45.5}\frac{\Gamma^2}{\beta}\left(\frac{E/Z}{10^{20}{\rm eV}}\right)^2 \,{\rm erg/s}, \quad (3)$$

where we have generalized the last equation to particles of charge Z.

Let us consider next the application of the general argument given above to the commonly assumed scenario,

where particle acceleration within the outflowing plasma is achieved via diffusive acceleration. In this case, one writes the acceleration timescale $t_{\mathrm{acc}} \equiv \mathcal{A} t_{\mathrm{L}}$ as a multiple $\mathcal{A}$ of the Larmor time, and one compares it to the dynamical timescale available for acceleration. Let us discuss this bound in some detail. For the sake of definiteness, we assume an outflow of Lorentz factor Γ and opening angle Θ (the isotropic case is recovered in the limit $\Theta^2 \to 2$). The quantity $\mathcal{A}$ depends on the diffusion coefficient of the particle, hence on its energy and the general properties of the magnetic field of the accelerating region. In acceleration mechanisms which involve scattering against magnetic inhomogeneities (such as Fermi I or Fermi II), $t_{\mathrm{acc}} \propto t_{\mathrm{s}}$, where $t_{\mathrm{s}} = 3\kappa/c$ is the scattering timescale and κ the diffusion coefficient. The parallel diffusion coefficient can be written as $\kappa/(r_{\mathrm{L}}c) \simeq \eta^{-1} (r_{\mathrm{L}}/\lambda_B)^{\alpha}$ (see for instance Casse, Lemoine & Pelletier 2002), with $\eta < 1$ the fraction of turbulent magnetic energy density (in units of total magnetic energy density) and λ_B the coherence length. The exponent α depends on the spectral index β of the (one dimensional) turbulence power spectrum: $\alpha = \beta - 1$ for $r_{\mathrm{L}} < \lambda_B$, $\alpha = 1$ for $r_{\mathrm{L}} > \lambda_B$. From this, one easily verifies that $\kappa/(r_{\mathrm{L}}c) > 1$ is general, meaning that the so-called Bohm regime $\kappa = r_{\mathrm{L}}c$ is a limiting regime. In non-relativistic Fermi shock acceleration ($\Gamma_{\mathrm{sh}}\beta_{\mathrm{sh}} \lesssim 1$ or $\beta_{\mathrm{sh}} \lesssim 0.7$), $t_{\mathrm{acc}} \simeq 3\kappa/\beta_{\mathrm{sh}}^2$, with β_{sh} the shock velocity in the comoving frame and κ refers to quantities measured in the upstream frame. Hence $\mathcal{A} \simeq 3\beta_{\mathrm{sh}}^{-2}\kappa/(r_{\mathrm{L}}c) \gg 1$. One recovers a similar result for non-relativistic Fermi II acceleration, with $\mathcal{A} \sim \beta_{\mathrm{A}}^{-2}\kappa/(r_{\mathrm{L}}c) \gg 1$, $\beta_{\mathrm{A}} < 1$ denoting the Alfvén speed. If acceleration takes place in a (non-relativistic) shear flow with velocity gradient $\Delta u/\Delta x$, the timescale $t_{\mathrm{acc}} \sim \Delta x^2/(\Delta u^2 t_{\mathrm{s}})$ (Rieger, Bosch-Ramon & Duffy 2007). The deconfinement limit corresponds to $t_{\mathrm{s}} \sim \Delta x/c$, in which case the limiting acceleration timescale becomes comparable to $t_{\mathrm{s}}c^2/\Delta u^2$, as above. Note that the acceleration timescale is larger (hence acceleration is less efficient) when $t_{\mathrm{s}} < \Delta x/c$. In the ultra-relativistic shock limit $\Gamma_{\mathrm{sh}}\beta_{\mathrm{sh}} \gg 10$, one expects $\mathcal{A} \simeq \Gamma_{\mathrm{sh}}^{-2}r_{\mathrm{L}}/\lambda_B$ (up to a factor of order unity, see Pelletier, Lemoine & Marcowith 2009), with the condition $r_{\mathrm{L}}/\lambda_B \gg \Gamma_{\mathrm{sh}}$. Since $\mathcal{A}$ increases with r_{L}, this process is in general not efficient. Finally, in the mildly relativistic regime $1 \lesssim \Gamma_{\mathrm{sh}}\beta_{\mathrm{sh}} \lesssim 10$, one expects $t_{\mathrm{acc}} \sim t_{\mathrm{s}}$, hence $\mathcal{A} \simeq \kappa/(r_{\mathrm{L}}c)$, whose minimum value is of order one provided the Bohm regime diffusion applies and the magnetic field is nearly fully turbulent.

To summarize, $\mathcal{A} \gg 1$ in general, and $\mathcal{A} \approx 1$ corresponds to a maximally efficient acceleration process. The constraint $t_{\mathrm{acc}} \leq t_{\mathrm{dyn}}$, with $t_{\mathrm{dyn}} = R/\beta\Gamma c$ the dynamical timescale at radius R (in the lab frame), now gives:

$$L_B \geq 0.65 \times 10^{45}\, \Theta^2 \Gamma^2 \mathcal{A}^2 \beta^3 Z^{-2} E_{20}^2 \,\mathrm{erg/s} \;, \quad (4)$$

with E_{20} the observed energy in units of $10^{20}\,\mathrm{eV}$. The presence of β^3 does not mean that in the limit $\beta \to 0$, this lower bound vanishes, since $\mathcal{A}^2 \propto \beta_{\mathrm{sh}}^{-4}$ more than compensates for this term. Similarly, the above bound does not vanish in the limit $\Theta \to 0$, since lateral escape losses become prominent when $\Theta < \Gamma^{-1}$. The corresponding timescale $t_{\mathrm{esc}} \simeq (\Theta R)^2/2\kappa$, hence $L_B \geq$

$1.2 \times 10^{45}\, \mathcal{A}\beta(\kappa/r_{\mathrm{L}}c)Z^{-2}E_{20}^2\,\mathrm{erg/s}$. In the case of AGN jets, one finds in general $\Theta\Gamma \sim 1$, hence both limits are comparable. According to the above discussion, the most optimistic values for the parameters entering these equations are $\beta \sim 1$, $\mathcal{A} \sim 1$ and $\kappa/(r_{\mathrm{L}}c) \sim 1$. Therefore $10^{45}Z^{-2}\,\mathrm{erg/s}$ can be considered as a firm lower bound on the source magnetic luminosity.

Since most of the AGN seen to correlate within $3°$ of the PAO events are Seyfert galaxies, with bolometric luminosities well below $10^{45}\,\mathrm{ergs/s}$, the AGN that they harbor cannot be the source of light particles at $10^{20}\,\mathrm{eV}$. We also note that Zaw, Farrar & Greene (2009) have shown that one third of this sample is actually made of star forming galaxies with little or no AGN activity. Hence the correlation with stricto-sensu AGN objects is actually weaker than reported.

Actually even FR I radio-galaxies, TeV blazars and BL Lac objects do not possess the required power to accelerate $Z \sim 1$ particles up to $10^{20}\,\mathrm{eV}$, since their magnetic luminosities are of order $L_B \sim 10^{42} - 10^{44}\,\mathrm{ergs/s}$ (Celotti & Ghisellini 2008). Such objects might possibly accelerate heavy nuclei up to energies around the GZK cut-off but, as discussed above, the anisotropy pattern at high and especially low energies would then appear inconsistent with the PAO results. Further anisotropy studies in both energy ranges would certainly further constrain their possible contribution.

The compilation of Celotti & Ghisellini (2008) has been done in the frame of leptonic synchrotron and inverse Compton emission. In hadronic blazar models, the magnetic field in the blazar zone is typically one order of magnitude larger than in leptonic models, so that these objects might fulfill the magnetic luminosity bound to accelerate protons up to $10^{20}\,\mathrm{eV}$. However, in this case, acceleration would occur in the blazar zone hence the emission should be beamed forward. In order to escape further expansion losses in the magnetized jets, the accelerated protons would have to be converted into neutrons, which would decay back to protons on a distance scale $\sim 0.9E_{20}\,\mathrm{Mpc}$, i.e. outside the jet. One should therefore observe a correlation of the arrival directions with blazars, not with radio-galaxies seen offside (Rachen 2008). However the Pierre Auger Observatory reports no correlation with blazars (Harari et al. 2007), so that this possibility is equally at odds with present observational results.

Keeping in line with the modelling of Celotti & Ghisellini (2008), only flat spectrum radio quasars (the likely equivalent to the most powerful FR II sources) seem capable of producing jets with $L_B > 10^{45}\,\mathrm{ergs/s}$. But, considering the highest energy PAO event ($E = 1.48 \pm 0.27 \pm 0.32 \times 10^{20}\,\mathrm{eV}$), one finds that the smallest angular separation of this event to the FR II sources located within 130 Mpc, as compiled by Massaglia (2007) is already $28°$ (for NGC 4261). The next objects are 3C 296 ($38°$ away) and PKS1343-60 ($41°$ away). The closest blazar (classified as BL Lac in the Véron & Véron-Cetty catalog) located closer than 150 Mpc lies $115°$ away from this highest energy event (TEX 0554+534).

Recently, it has been proposed that transients in active galactic nuclei could power up the engine up to the luminosities required, thereby evading the above constraints (see for instance Farrar & Gruzinov 2009, Dermer et al.

2008). However, as demonstrated by Waxman & Loeb (2009), such transients should produce counterpart flares in X-rays through the concomittant acceleration of electrons, which should have been picked up by existing surveys. Their non-detection strongly argues against such flaring scenarios.

4.2. *The particular case of Cen A*

Given its proximity and the apparent clustering of PAO events in this direction of the sky, Cen A has received a lot of attention. In particular, several authors have suggested that this AGN could host a site of acceleration to ultra-high energies (Cavallo 1978; Romero et al. 1996; Farrar & Piran 2000; Gorbunov et al. 2008; Hardcastle et al. 2009, O'Sullivan, Reville & Taylor 2009). Let us therefore discuss it in some more detail.

Centaurus A is classified as a FR I / misaligned blazar (see Israel 1998 for a review). Its bolometric luminosity $L_{\rm bol} \sim 10^{43}$ erg/s and its jet kinetic power is inferred to be $L_{\rm jet} \simeq 2 \times 10^{43}$ erg/s. Therefore, this source should not be able to accelerate light particles to 10^{20} eV. The detailed modelling of the spectral energy distribution of its nucleus by Chiaberge, Capetti & Celotti (2001) provides further information on the emission zone: $R \sim 10^{16}$ cm, $B \sim 0.5$ G and $\Gamma \leq 3 - 5$. This corresponds to a magnetic luminosity $L_B = \frac{1}{4}R^2B^2\Gamma^2\beta c \sim 2 \times 10^{42}$ ergs/s, a value that seems quite reasonable in view of the jet kinetic power and of the bolometric luminosity, and which agrees relatively well with estimates of the magnetic field in the inner jet at larger distances from the core, when assuming $BR \sim$ constant.

The papers which have discussed the issue of acceleration to ultra-high energy in some detail are Romero et al. (1996), which has argued that acceleration can take place in the X-ray knots of the inner jet through diffuse shock acceleration, Hardcastle et al. (2009) and O'Sullivan, Reville & Taylor (2009), which have discussed the stochastic acceleration of protons in the giant lobes of Cen A and Gorbunov et al. (2008) relying on the model of Neronov et al. (2007) of particle acceleration in a black hole magnetosphere.

Romero et al. (1996) uses the inferred values of $B \simeq 10^{-5}$ G (upstream field), $R \simeq 1.8$ kpc, $\beta_{\rm sh} \simeq 0.3$ and $\eta \simeq 0.4$. However, since the Larmor radius $r_{\rm L} \simeq 11$ kpc $E_{20}Z^{-1}B_{-5}^{-1} > R$ (with $E_{20} = E/10^{20}$ eV, $B_{-5} = B/10^{-5}$ G), even the Hillas criterion (Hillas 1984) is not satisfied. Balancing the acceleration timescale with the escape timescale R/c, one derives a maximal energy $E \lesssim 10^{18} Z\beta_{0.3}^2 B_{-5}R_{1.8}$ eV ($R_{1.8} \equiv R/1.8$ kpc, $\beta_{0.3} \equiv \beta_{\rm sh}/0.3$). As discussed above, this maximal energy lies in the correct ballpark for accelerating nuclei to ultra-high energies. However the anisotropy signal would then appear incompatible with the PAO data; in particular, a strong anisotropy signal at EeV energies should have been detected.

Hardcastle et al. (2009) have argued that protons could be accelerated up to $\sim 5 \times 10^{19}$ eV through stochastic acceleration in the magnetized turbulence of the giant lobes of Cen A. However, one can show that their estimate of the acceleration timescale is far too optimistic because, when applied to the electrons, it produces a maximal energy well in excess of the inferred

$E_{\rm max,e} \sim 1 - 4 \times 10^{11}$ eV. In detail, using the estimate of Hardcastle et al. (2009) for the acceleration timescale, $t_{\rm acc} \simeq 3.5 \times 10^6$ yrs $E_{20}B_{-6}^{-1}$, and their Bohm scaling $t_{\rm acc} \propto E$, one infers the maximal energy for electrons by comparing $t_{\rm acc}$ to the synchrotron and inverse Compton energy loss timescales, leading to $E_{\rm max,e} \sim 2 \times 10^{16} B_{-6}^{-1/2}$ eV. The above maximal electron energy is five orders of magnitude larger than the inferred maximal energy, hence the above acceleration timescale is far too optimistic and, consequently, the maximal proton energy must be much lower than 10^{20} eV. This conclusion agrees with those of O'Sullivan, Reville & Taylor (2009); see also Casse, Lemoine & Pelletier (2002) for a similar discussion regarding the acceleration in the lobes of powerful radio-galaxies.

Finally, Neronov et al. (2007) have argued that in a magnetic field of strength $B = 10^4$ G threading a maximally rotating black hole of mass $M_{\rm bh} = 10^8\,M_\odot$, heavy nuclei could be accelerated to energies of order 10^{20} eV by exploiting the potential drop $\Phi \simeq 10^{20}B_4M_8$ V. However, this maximal energy is quite optimistic because it ignores radiative energy losses, which are highly efficient in the nuclei of powerful AGN (Norman et al. 1995, Henri et al. 1999). In any case, the Poynting flux that is required, $L_{\rm B} \sim 10^{45}$ erg/s far exceeds any other luminosity measured elsewhere in the galaxy, and in particular the estimate obtained from multi-band spectral modelling of the nucleus emission (Chiaberge, Capetti & Celotti 2001).

5. DISCUSSION

5.1. *Summary*

Let us start by summarizing the results obtained so far. We have discussed how one can can test the chemical composition of ultra-high rays on the sky by comparing the anisotropy signals at various energies. Our main result is to show that if anisotropies are observed above some energy $E_{\rm thr}$ and the composition is assumed to be heavy at that energy (nuclei of charge Z), one should observe at energies $> E_{\rm thr}/Z$ a substantially stronger anisotropy signal, which is associated with the proton component emitted by the sources that are responsible for the anisotropy pattern. These conclusions do not depend at all on the modelling of the intervening magnetic fields and they are robust with respect to the parameters characterizing the sources.

We have then applied this test to the most recent data of the PAO. We find that, if these data are taken at face value (and if the PAO arrival directions around the ankle appear isotropic), the events that are responsible for the anisotropy signal reported toward Cen A and toward the nearby AGN should not be heavy nuclei. Interestingly, this result appears to be at odds with the current PAO results on the chemical composition at the highest energies. One cannot exclude at the present time that the observed anisotropies are statistical accidents; only the acquisition of a larger set of data will tell. One cannot exclude either that the composition switches abruptly from heavy to light at ~ 30 EeV. Finally, one cannot exclude that a systematic bias affects the composition measurements of the PAO. In any case, the present discussion indicates that, if both the anisotropy and the heavy composition are confirmed by future data, some

possibly important information is to be extracted out of this apparent contradiction.

The theoretical and experimental uncertainties in the extrapolation of the $p - p$ cross-section to center-of-mass energies $\sqrt{s} \gtrsim 100\,\mathrm{TeV}$ are one of the possible sources of biases in shower reconstruction. Recently, it has been argued that, if this cross-section were underestimated by some $40 - 60\,\%$ at these energies, one might reconcile the existing $X_{\max}$ measurements with a pure proton composition at energies above the ankle (Ulrich et al. 2009a, 2009b; see however Wibig 2009). In this respect, and in the light of the above discussion, the apparent anisotropy towards Cen A offers a very valuable opportunity to test this possibility. It suffices, in principle, to test the anisotropy pattern against a future (independent) data set at various energies by comparing the number of events detected within a predetermined solid angle in a predetermined direction to the expected number for isotropic arrival directions; at the same time, one needs to perform a dedicated composition measurement for cosmic rays from this particular region of the sky, in order to avoid as much as possible the contamination due to the isotropic contribution to the all-sky flux. Then, one should apply the test discussed above.

5.2. The interpretation of the PAO data

The natural question that follows is what can be inferred about the sources of ultra-high energy cosmic rays if, following the anisotropy results of PAO and the above discussion, one assumes that most ultra-high energy cosmic rays are protons. Let us now explore this line of reasoning.

First of all, one concludes that the existing data of the PAO disfavor the AGN model of ultra-high energy cosmic ray origin. Indeed, we have discussed in Section 4 a robust lower bound to the magnetic luminosity that a source must possess in order to be able to accelerate particles of charge Z up to $10^{20}\,\mathrm{eV}$, $L_B \gtrsim 10^{45}\,Z^{-2}\,\mathrm{erg/s}$. This bound allows to rule out the local radio quiet AGN as sources of $10^{20}\,\mathrm{eV}$ protons. We have also argued that, while FR I radio-galaxies do not seem to possess the required luminosity to accelerate protons up to $10^{20}\,\mathrm{eV}$, FR II radio-galaxies and blazars do not correlate with the highest energy events. Although radio-loud galaxies could possibly accelerate heavy nuclei up to energies close to the GZK cut-off, as we have discussed they would produce an anisotropy pattern predominantly at $\sim \mathrm{EeV}$ energies rather than at ultra-high energies, in conflict with the PAO results.

We have discussed the particular case of Cen A in some detail, as this source has recently received a lot of attention due to the observed clustering of events around it. We have provided a critical discussion of acceleration in this object and argued that its AGN/jet/lobe system cannot produce protons at the energies required, in good agreement with the general expectations from the above luminosity bound. That being said, the excess clustering in this particular direction, if real, remains to be interpreted.

First, if sources are distributed according to the large scale structure, one expects a certain number of events to coincide accidentally with the direction of Cen A, because of the location of the Centaurus and Shapley superclusters in this direction. Using the PSCz catalog of galaxies as a proxy for the distribution of the sources, with a depth of $200\,\mathrm{Mpc}$, and accounting for the PAO exposure, one expects 0.80 events above $55\,\mathrm{EeV}$ within $6°$ of Cen A nucleus (and 0.3 for isotropic arrival directions) for $2 - 3$ observed, or 4.4 events within $18°$ (and 2.7 for isotropic arrival directions) for 12 observed. Note that the large scale structure is poorly sampled in the proximity of Cen A due to its low galactic latitude. Nevertheless, the above numbers already indicate that the contamination from the surrounding large scale structure in the direction to Cen A is substantial. In particular, at the present level of statistics, one cannot claim observing a significant departure from a model in which the sources are distributed as the large scale structure. It should also be recalled here that the PAO analysis of clustering around Cen A is an a posteriori one, hence one may not therefore assign a reliable significance to the detection of the anisotropy.

Moreover, if sources are gamma-ray bursts or magnetars, one should include in the flux prediction the contribution of such sources located in the Cen A host galaxy itself. It is well known that the probability of detecting ultra-high energy cosmic rays from nearby gamma-ray bursts is extremely small unless the arrival times of these ultra-high energy cosmic rays are sufficiently dispersed (Waxman 1995, Waxman & Miralda-Escudé 1996). Consider for instance gamma-ray bursts with rate of occurence $\dot{N}_{\mathrm{GRB}}$ in Cen A; these can be seen if either of their jets points into a solid angle $2\pi(1 - \cos\delta\theta)$ where $\delta\theta$ is the typical deflection acquired by the cosmic ray en route to the detector, giving a detection probability $P \sim \dot{N}_{\mathrm{GRB}}\sigma_t\delta\theta^2/2 \sim 10^{-4}\dot{N}_{\mathrm{GRB},-5}E_{70}^{-4}B_{-8}^4\lambda_{100\mathrm{kpc}}^2$, with $\dot{N}_{\mathrm{GRB}} = 10^{-5}\dot{N}_{\mathrm{GRB},-5}\,\mathrm{yr}^{-1}$; $\sigma_t = 6 \times 10^3\,\mathrm{yr}\,B_{-8}^2\lambda_{100\mathrm{kpc}}E_{70}^{-2}$ represents the spread of arrival times and $\delta\theta = 3°B_{-8}\lambda_{100\mathrm{kpc}}^{1/2}E_{70}^{-1}$ the angular deflection for particles of energy $E = 70\,E_{70}\,\mathrm{EeV}$ traveling from Cen A to the detector through a magnetic field of strength $10^{-8}B_{-8}\,\mathrm{G}$ and coherence length $100\,\lambda_{100\,\mathrm{kpc}}\,\mathrm{kpc}$ (Waxman & Miralda-Escudé 1996). The above probability suggests that one should not detect events from gamma-ray bursts emitted directly toward the observed. However, if the jet of the gamma-ray burst hits one of the lobes of Cen A, the particles can be redistributed in all directions, in particular towards the detector. The magnetic field inside the lobe, $B \sim 1\,\mu\mathrm{G}$ is indeed sufficient to impart a deflection of order unity on the lobe distance scale $\sim 100\,\mathrm{kpc}$ to protons of $70\,\mathrm{EeV}$. In this case, the expected time delay and time dispersion are of the order of the travel time to the lobes, $L_{\mathrm{lobes}}/c \sim 3 \times 10^5\,\mathrm{yr}$, so that the expected number of gamma-ray bursts that one can see at any time, through rescattering of the particles on the lobes of Cen A is:

$$\langle N_{\mathrm{GRB}} \rangle \simeq \dot{N}_{\mathrm{GRB}} \frac{L_{\mathrm{lobes}}}{c} \frac{\Delta\Omega_{\mathrm{lobes}}}{2\pi} \sim \mathcal{O}(1)\dot{N}_{\mathrm{GRB},-5} \quad (5)$$

for an apparent solid angle of the lobes $\Delta\Omega_{\mathrm{lobes}}$ as viewed from the host galaxy of Cen A, which is close to 4π.

The last gamma-ray burst(s) of Cen A may then contribute to the flux above the GZK cut-off up to:

$$j_{\mathrm{Cen\,A}} \approx 0.9{\times}10^{-41}\,\mathrm{eV}^{-1}\mathrm{cm}^{-2}\mathrm{s}^{-1}\,\epsilon_{51}E_{70}^{-2}f_\epsilon^{-1}\sigma_{t,5.5}^{-1}\langle N_{\mathrm{GRB}}\rangle\,, \quad (6)$$

with $\sigma_{t,5.5} = \sigma_t/3 \times 10^5$ yrs, $f_\epsilon = \ln(E_{\max}/E_{\min}) \sim 1 - 10$ for an injection spectrum with $s = 2.0$, and $\epsilon = 10^{51}\epsilon_{51}$ ergs the energy injected by one gamma-ray burst in ultra-high energy cosmic rays. This flux should be spread over the angular scale of the lobes, $\sim 10°$. At 70 EeV, PAO records a diffuse flux $j_{\mathrm{PAO}}(70\,\mathrm{EeV}) \simeq 3 \times 10^{-40}\,\mathrm{eV}^{-1}\mathrm{cm}^{-2}\mathrm{s}^{-1}\mathrm{sr}^{-1}$. After correcting for the solid angle of the Cen A image and the PAO aperture towards Cen A, one finds that the last gamma-ray bursts in Cen A should contribute up to $2 - 25\%$ of the observed PAO flux, well within the range of the observed anisotropy.

We also note that this contribution from sources inside Cen A would improve the overall correlation of all the PAO data above 55 EeV with sources distributed as the local large scale structure. Finally, we remark that the above effect of rescattering on the lobes provides a clear example of the possible biases discussed in Kotera & Lemoine (2008), namely that the PAO could be preferentially observing the last scattering centers (in the present case, the lobes of Cen A) rather than the source itself (the gamma-ray bursts located in the core of Cen A).

REFERENCES

Abbasi, R. U., et al. (The HiRes Collaboration), 2004, ApJ, 610, L73

Abbasi, R. U., et al. (The HiRes Collaboration), 2005, ApJ, 623, 164

Abbasi, R. U., et al. (The HiRes Collaboration), 2008, Physical Review Letters, 100, 101101

Abraham, J. et al. (The Pierre Auger Collaboration), 2007, Science, 318, 938

Abraham, J., et al. (The Pierre Auger Collaboration), 2008a, Physical Review Letters, 101, 061101

Abraham, J. et al. (The Pierre Auger Collaboration), 2008b, Astroparticle Physics, 29, 188

Allard, D., Busca, N. G., Decerprit, G., Olinto, A. V., & Parizot, E. 2008, Journal of Cosmology and Astro-Particle Physics, 10, 33

Allard, D., & Protheroe, R. J. 2009, arXiv:0902.4538

Aloisio, R., Berezinsky, V., & Gazizov, A. 2008, arXiv:0803.2494

Arons, J. 2003, ApJ, 589, 871

Belz, J. (The HiRes Collaboration), *proc. CRIS-2008* (Malfa, Italy, Sept. 2008)

Aublin, J. et al. (The Pierre Auger Collaboration), 2009, arXiv:0906.2347, ICRC 2009

Bertone, G., Isola, C., Lemoine, M., & Sigl, G. 2002, Phys. Rev. D, 66, 103003

Casse, F., Lemoine, M., & Pelletier, G. 2002, Phys. Rev. D, 65, 023002

Cavallo, G. 1978, A&A, 65, 415

Celotti, A., Ghisellini, G., 2008, MNRAS, 385, 283

Chiaberge, M., Capetti, A., & Celotti, A. 2001, MNRAS, 324, L33

Cuoco, A., & Hannestad, S. 2008, Phys. Rev. D, 78, 023007

Dermer, C. D., Razzaque, S., Finke, J. D., & Atoyan, A., 2008, arXiv:0811.1160

Evans, N. W., Ferrer, F., Sarkar, S., 2003, PRD 69, 3501.

Evans, N. W., Ferrer, F., Sarkar, S., 2004, PRD 69, 8302.

Farrar, G. R., & Piran, T. 2000, arXiv:astro-ph/0010370

Farrar, G. R., Berlind, A. A., & Hogg, D. W. 2006, ApJ, 642, L89

Farrar, G. R., & Gruzinov, A., 2009, ApJ, 693, 329

Finley, C. B., & Westerhoff, S. 2004, Astroparticle Physics, 21, 359

Ghisellini, G., Ghirlanda, G., Tavecchio, F., Fraternali, F., & Pareschi, G. 2008, arXiv:0806.2393

Gorbunov, D. S., Tinyakov, P. G., Tkachev, I. I., Troitsky, S. V., 2002, ApJ 577, L93.

Gorbunov, D. S., Tinyakov, P. G., Tkachev, I. I., Troitsky, S. V., 2004, `astro-ph/0406654`.

Gorbunov, D. S., Tinyakov, P. G., Tkachev, I. I., & Troitsky, S. V. 2008, arXiv:0804.1088

Greisen, K., 1966, PRL 16, 748.

Gupta, N. 2008, Journal of Cosmology and Astro-Particle Physics, 6, 22

Hague, J. D. et al. (The Pierre Auger Collaboration), arXiv:0906.2347, ICRC 2009

Halzen, F., & O'Murchadha, A. 2008, arXiv:0802.0887

Harari, D., et al. (The Pierre Auger Collaboration), 2007, arXiv:0706.1715

Hardcastle, M. J., Cheung, C. C., Feain, I. J., & Stawarz, L. 2009, MNRAS, 393, 1041

Henri, G., Pelletier, G., Petrucci, P. O., & Renaud, N. 1999, Astroparticle Physics, 11, 347

Hillas, A. M. 1984, ARA&A, 22, 425

Holder, J., & for the VERITAS Collaboration 2008, arXiv:0810.0471

Israel, F. P. 1998, A&A Rev., 8, 237

Kachelriess, M., Ostapchenko, S., & Tomas, R. 2008, arXiv:0805.2608

Kashti, T., & Waxman, E. 2008, Journal of Cosmology and Astro-Particle Physics, 5, 6

Kotera, K., & Lemoine, M. 2008, Phys. Rev. D, 77, 123003

Lyutikov, M., & Ouyed, R. 2005, arXiv:astro-ph/0507620

Massaglia, S., 2007, Nuc. Phys. B Proc. Supp. 168, 302

Milgrom, M., & Usov, V. 1995, ApJ, 449, L37

Moskalenko, I. V., Stawarz, L., Porter, T. A., & Cheung, C. C. 2008, arXiv:0805.1260

Nagar, N. M., & Matulich, J. 2008, arXiv:0806.3220

Neronov, A., Semikoz, D., & Tkachev, I. 2007, arXiv:0712.1737

Norman, C. A., Melrose, D. B., & Achterberg, A. 1995, ApJ, 454, 60

O'Sullivan, S., Reville, B., & Taylor, A. M., 2009, arXiv:0903.1259

Pelletier, G., Lemoine, M., & Marcowith, A., 2008, arXiv:0707.3459

Panov, A. D., et al. (ATIC-2 Collaboration) 2006, arXiv:astro-ph/0612377

Rachen, J. P., & Biermann, P. L. 1993, A&A, 272, 161

Rachen, J., 2008, in Proceedings of "Rencontres de Blois 2008 - Challenges in particle astrophysics", Blois (France), May 18-23 2008, ed. J. Dumarchez

Rieger, F. M., Bosch-Ramon, V., & Duffy, P. 2007, Ap&SS, 309, 119

Romero, G. E., Combi, J. A., Perez Bergliaffa, S. E., & Anchordoqui, L. A. 1996, Astroparticle Physics, 5, 279

Saunders, W., Frenk, C., Rowan-Robinson, M., Lawrence, A., & Efstathiou, G. 1991, Nature, 349, 32

Stanev, T., Biermann, P. L., LLoyd-Evans, J., Rachen, J. P., Watson, A. A., 1995, PRL 75, 3056.

Takeda, M., et al. 1999, ApJ, 522, 225

Tinyakov, P. G., Tkachev, I. I., 2001, Pisma Zh. Eksp. Teor. Fiz. 74, 3 [JETP Lett. 74, 1].

Tinyakov, P. G., Tkachev, I. I., 2002, Astropart. Phys. 18, 165.

Tinyakov, P. G., Tkachev, I. I., 2004, PRD 69, 8301.

Uchihori, Y., Nagano, M., Takeda, M., Teshima, M., LLoyd-Evans, J., Watson, A. A., 2000, Astropart. Phys. 13, 151.

Ulrich, R., Engel, R., Müller, S., Pierog, T., Schüssler, F., & Unger, M. 2009a, arXiv:0906.0418

Ulrich, R., Engel, R., Müller, S., Schüssler, F., & Unger, M. 2009b, arXiv:0906.3075

Unger, M. et al. (The Pierre Auger Collaboration), ICRC-2007, arXiv:0706.1495

Véron-Cetty, M.-P., & Véron, P. 2006, A&A, 455, 773

Vietri, M. 1995, ApJ, 453, 883

Wahlberg, H. et al. (The Pierre Auger Collaboration), 2009, arXiv:0906.2319, ICRC 2009

Waxman, E. 1995, Phys. Rev. Lett., 75, 386.

Waxman, E., & Miralda-Escudé, J. 1996, ApJ, 472, L89

Waxman, E., 2005, Phys. Scripta, T121, 147

Waxman, E., & Loeb, A., 2008, arXiv:0809.3788

Wibig, T. 2008, arXiv:0810.5281

Wibig, T. 2009, Phys. Rev. D, 79, 094008

Yamamoto, T. et al. (The Pierre Auger Collaboration), ICRC 2007

Zatsepin, G. T., Kuzmin, V. A., 1966, Pis'ma Zh. Eksp. Teor. Fiz. 4, 114 [JETP. Lett. 4, 78].

Zaw, I., Farrar, G. R., & Greene, J. E. 2009, ApJ, 696, 1218